Modeling Turbulent Enhancement of Sediment Transport

Basic Information

Title:	Modeling Turbulent Enhancement of Sediment Transport
Project Number:	2009LA60B
Start Date:	3/1/2009
End Date:	9/30/2010
Funding Source:	104B
Congressional District:	6th
Research Category:	Climate and Hydrologic Processes
Focus Category:	Sediments, Geomorphological Processes, Water Quantity
Descriptors:	
Principal Investigators:	Heather Smith

Publications

There are no publications.

Project Title: Modeling Turbulent Enhancement of Sediment Transport
Project Number:
Start Date: March 1, 2009
End Date: February 29, 2010
Congressional District: 6
Focus Categories: Sediments, Geomorphological and Geochemical Processes
Principal Investigator: Heather D. Smith

Research Objectives

The State of Louisiana faces serious challenges with coastal erosion and subsidence. Restoration efforts have been focused on the ability to use sediment available from the Mississippi River to increase land building in vulnerable wetland areas. It is believed that by increasing the wetlands around the coast, storm surge can be reduced[1]. Additionally, increased sea level rise, combined with large recurring hurricanes will increase the potential to resuspend sediments that may have been contaminated and buried. The interactions at the interface of the sediment bed and fluid is one of the largest challenges still to be resolved in water resources. Our ability to predict sediment transport at large scales is limited by our understanding of the physics dominating sediment movement in a variety of complex forcing regimes. In addition, the characteristics of the sediment material is difficult to assess and parametrize.

The role of externally generated turbulence on local sediment transport continues to be an active area of research. Detailed laboratory experiments have been performed to investigate the effect of externally generated turbulence on bed load transport. Nelson *et al.* (1993) made detailed flow measurements around fixed two-dimensional bedforms. The authors observed that the mean bed shear stress close to the reattachment point on the lee side of a ripple continually remained below the threshold for incipient motion. Sediment motion occurs due to the presence of excess turbulence generated as a result of the flow separation. This work was further extended to the case of turbulence generated from a backward facing step. Nelson *et al.* (1995) found a strong correlation between the sediment motion and the near bed velocity fluctuations. Sumer *et al.* (2003) reported experiments performed with externally generated turbulence due to the presence of obstacles in the flow. The investigators considered the turbulence generated by large and small screens and a two-dimensional pipeline. For these experiments, the applied stress by the flow was maintained at a level low enough to produce bed load transport only without the formation of bedforms. The bed load transport rate correlated very well to the turbulent intensity. A 20% increase in local turbulence levels in the bed shear stress increased the bed load sediment transport rate by a factor of 6. The bed load transport rate was found to be insensitive to the turbulence generation mechanism (whether screens or cylinder), and only sensitive to the turbulence level. The spectrum width of the externally generated turbulence (such as the frequency of the vortex shedding) did not have a significant effect on the resulting sediment transport.

The goal of this research is to investigate the effect of turbulence on the applied shear, and thus the resulting sediment transport. The necessity to resolve the time-varying hydrody-

[1]Louisiana Coastal Protection and Restoration Draft Report - http://lacpr.usace.army.mil

namics and turbulence in sediment transport modeling efforts has been shown for a variety of applications, including the scour around pipelines (Sumer *et al.*, 1988; Li and Cheng, 2001), dunes (Tjerry and Fredsøe, 2005; Giri and Shimizu, 2006), and coastal bedforms (Nichols and Foster, 2007). This numerical work will consider the hydrodynamics around a bottom-mounted cylinder undergoing sinusoidal wave forcing. Three parametrization for the numerical prediction of turbulence will be investigated, the two-equation k-ϵ and two versions of the damped Smagorinsky Large Eddy Simulation (LES) closure schemes. The modeled bed stress and external flow field will be compared with a variety of available laboratory data.

Objectives

Objective 1: Compare the hydrodynamics around the cylinder in waves

In this objective, we will simulate the vortex generation and shedding around a bottom-mounted cylinder for three turbulence closure schemes, two surface roughness values, and two grid sizes. Predictions of the lift coefficient, Cl will be compared to available laboratory data of Sumer *et al.* (1991) and Bryndum *et al.* (1992).

Objective 2: Compare the phase-dependent estimates of the applied bed shear

Estimates of the applied bed shear stress will be determined as a function of wave phase for the simulations of Objective 1. These predictions of the shear will be compared to the data obtained by Sumer and Fredsøe (1991). The role of the turbulent eddy viscosity in the predictions of the stress will yield important information on the appropriateness of the turbulence model as well as the spatially- and temporally-varying applied shear.

Methodology

Model Specifics

In this research, we utilize the three-dimensional, non-hydrostatic, commercially available model, FLOW-3D. This model utilizes a Volume of Fluid (VOF) approach to resolve fluid-fluid and fluid-boundary interfaces by tracking curvature and location of the interfaces in a cell (Richardson and Panchang, 1998; Hirt, 1993). This allows rectangular non-boundary fitted grid cells to resolve complex flow and obstacle features.

The model simultaneously solves the three-dimensional Navier-Stokes equations and the continuity equation. Pressure is calculated through the solution of the pressure Poisson equation through an iterative procedure. The contributions of the turbulence are included with the addition of a kinematic eddy viscosity, μ_T. The turbulence models proposed in this research are the two-equation k-ϵ and the Large Eddy Simulation (LES) closure schemes. The standard k-ϵ model (Wilcox, 2002) approximates the kinematic eddy viscosity with

$$\mu_T = \frac{\rho C_\mu k^2}{\epsilon} \tag{1}$$

The closure equations for the turbulent kinetic energy, k, and the dissipation rate, ϵ are solved with standard transport equations. The boundary conditions for k and ϵ are given as

$$k = \frac{u_*^2}{\sqrt{C_\mu}}, \qquad \epsilon = \frac{u_*^3}{\kappa y_o} \tag{2}$$

The non-transport turbulence closure scheme that will be considered is the Large Eddy Simulation (LES). The equation for the kinematic eddy viscosity, μ_T, is given by (3)

$$\mu_T = \rho(C_{s,d}\Delta)^2\sqrt{2e_{ij}e_{ij}} \tag{3}$$

where the strain-rate tensor e_{ij} is given by

$$e_{ij} = \left(\frac{\partial u_i}{\partial x_j} + \frac{\partial u_j}{\partial x_i}\right) \tag{4}$$

The characteristic length scale, Δ, is

$$\Delta = (\delta x \delta y \delta z)^{1/3} \tag{5}$$

Near the wall, this length scale is modified to account for the limitations of the Smagorinsky closure scheme with a van Driest damping term, $C_{s,d}$, given with

$$C_{s,d} = C_s\left[1 - \exp\left(-\left(z_+/A_+\right)^n\right)\right]^m$$

where C_s is a coefficient equal to 0.1 and A_+ has a value of 25. Two formulations for van Driest damping are considered here. The first is the standard form where $n = 1$ and $m = 1$. A second form proposed by Guerts (2004), where $n = 3$ and $m = 0.5$. In numerical models, the applied bed stress can be calculated with either a law of the wall function, or the fundamental definition of the bed shear stress, which assumes adequate resolution of the viscous sublayer. In either approach, the contribution of the turbulence closure scheme is achieved through the use of the total viscosity in the calculation. The total viscosity is defined as

$$\mu_{tot} = \mu + \mu_T \tag{6}$$

This approach will consider both formations of the bed shear stress and the sensitivity of the stress to the inclusion of the turbulent component.

Laboratory Experiments

In this investigation, we perform model-data comparisons with laboratory data obtained by Sumer and Fredsøe (1991). In their work, the applied shear stress and the bed was measured at several streamwise locations around a 5 cm diameter cylinder with flush-mounted hot-film probes in an oscillatory U-tube. The cylinder was mounted directly onto the bed. The wave forcing had a period of 9.8 s and a maximum freestream velocity of 5.2 cm/s, yielding a Keulegan-Carpenter number of approximately 10. Values of the lift coefficient for this Keulegan-Carpenter number are based on ranges published in Sumer *et al.* (1991) and Bryndum *et al.* (1992).

For the numeric simulations, a domain size of 120 cm by 35 cm was resolved with a two different grid sizes, a variable 0.125 cm and a variable 0.0625 cm grid. The Stokes length of the wave bottom boundary layer is approximately 0.18 cm, yielding nearly 2 cells covering the boundary layer for a 0.125 cm grid and 3 cells covering the boundary layer for a 0.0625 cm grid. Both girds have a constant cell size in the vicinity of the cylinder and then the cell size expands linearly toward the domain ends (with an expansion ratio less than 1.25). Two values for obstacle and bed roughness were considered (0.008 and 0.016 cm).

Results

Lift Predictions

The vortex dynamics around obstacles in waves is dominated by the strength and duration of the forcing. Figure 1 presents the vortex dynamics around the cylinder as visualized with the vorticity for the LES $n = 1$ model (left panels) and k-ϵ model (right panels). A vortex is generated in the lee of the cylinder during times with low accelerations. As the flow starts to reverse, the vortex separates from the cylinder and flips over top of the cylinder. As the flow continues in the opposite direction, the flipped vortex continues to move away from the cylinder and a new lee vortex is generated. At this point, two very distinct differences are observed with the LES $n = 1$ and k-ϵ predictions. The LES $n = 1$ model predicts a vortex pair that couples and sheds from the cylinder during flow reversal. This coupling is not observed with the k-ϵ model. The LES $n = 1$ model also predicts remnants of previously flipped vortices that are still observable in the flow for several wave periods. This is consistent with other observations of the vortex dynamics around bottom-seated cylinders.

Model evaluation of both the k-ϵ and LES closure schemes of the vortex generation and shedding properties are performed with the lift coefficient. Laboratory data for the lift coefficient was obtained by both Sumer *et al.* (1991) and Bryndum *et al.* (1992). Figure 2 presents the range of parameters (grid size, roughness, damping type) for the LES models considered. Figure 3 presents the comparison of the k-ϵ and LES $n = 1$ models. As the flow reverses, the low pressure vortex core passes over the top of the cylinder, yielding a peak in the lift coefficient. This occurs twice per wave period. The lift coefficients predicted by the LES models are lower than expected for the finer grid and are improved by increasing the grid size. Neither LES or k-ϵ coarse grid models show much sensitivity to the roughness value. The k-ϵ model does not appear to be as sensitive to grid size as the LES models. While the magnitude predictions of k-ϵ model are more consistent with the data, the LES models is able to more accurately capture the secondary lift peak associated with the shedding of the vortex pair.

Bed Stress Predictions

The highly dynamic nature of the flow around the cylinder is expected to have a significant impact on the predictions of the bed shear stress. Figure 4 and Figure 5 present the comparisons of the predicted bed shear stress with those observed by Sumer and Fredsøe (1991). The bed stress was calculated with the formulas presented in the model section in the cell nearest to the boundary and used the total turbulent viscosity ($\mu_{tot} = \mu + \mu_T$). The magnitudes of the bed stress are reasonably well predicted with the LES models. Near the cylinder, the models agree with each other fairly well, indicating that the model in the region of the cylinder is not important. The higher damping produced with the LES $n = 3$ model provides better agreement in the far field stress predictions than that with the LES $n = 1$ model. The interactions of the bed with remnant vortices are observed in the far-field region ($|x/D| > 5$). The magnitude of the stress in these areas are not dependent on the grid size, but the spatial location of the peaks differ, indicating that the hydrodynamics may be different between models. The contributions of these large, temporally varying local bed stresses on the sediment transport would be considerable, and not considered with models unable of resolving these features.

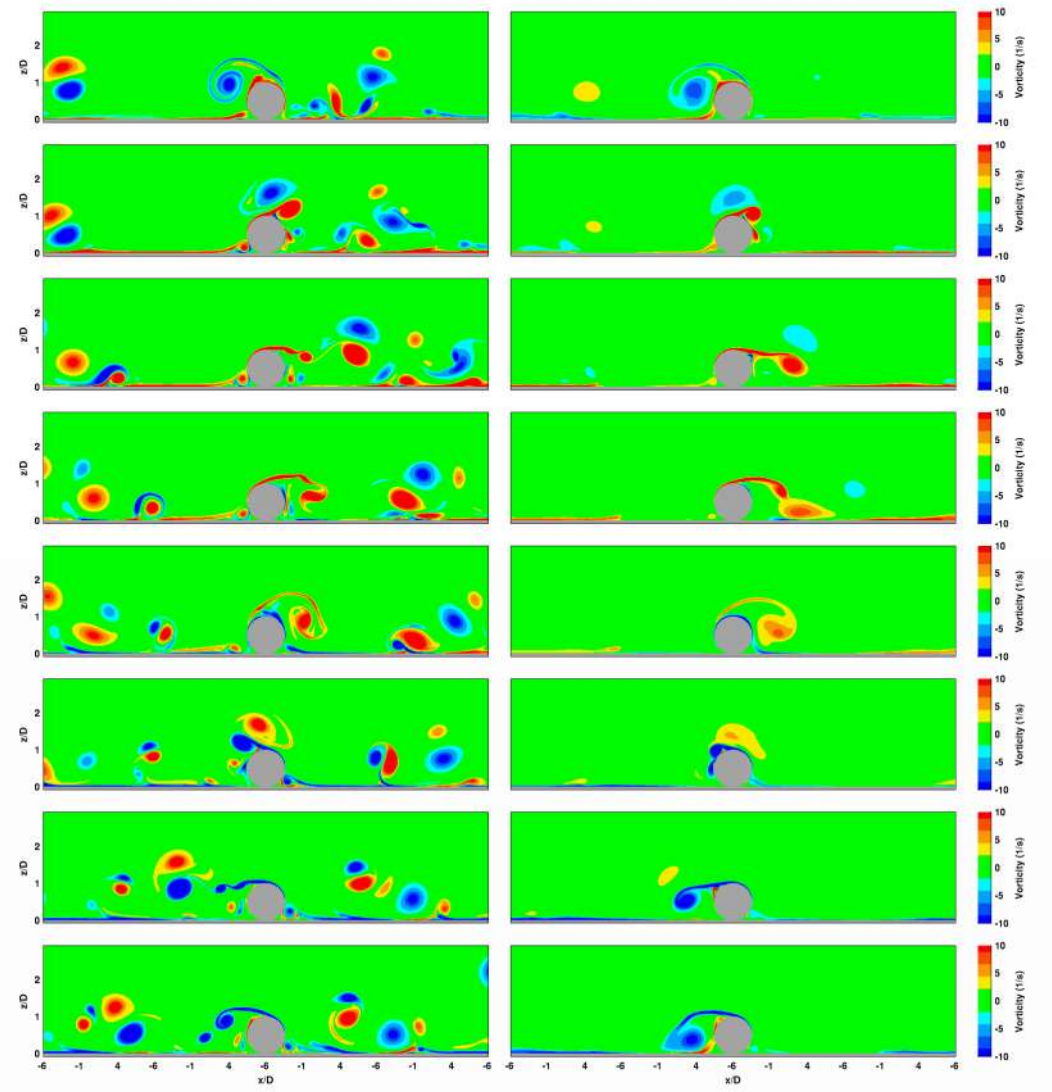

Figure 1: Modeled vorticity for the LES model ($n = 1$, left panels) and the k-ϵ model (right panels) for the finer grid and a roughness of 0.008 cm. Color scaling for the vorticity is shown on the right, with red indicating clockwise rotation. The temporal location for each panel is given at the top.

Predictions of the bed shear stress when considering the k-ϵ model are dramatically different than both those predicted with the LES closure scheme and the laboratory data (Figure 5). The predicted bed stress is several times larger than the laboratory observations. The far-field stress is well-predicted during some of the wave phases, but in general, it is over-predicted as well. The difference in the strength of the predicted vortices is also apparent. The k-ϵ model does not show the local peaks in the bed shear stress that indicate the presence of previously shed vortices.

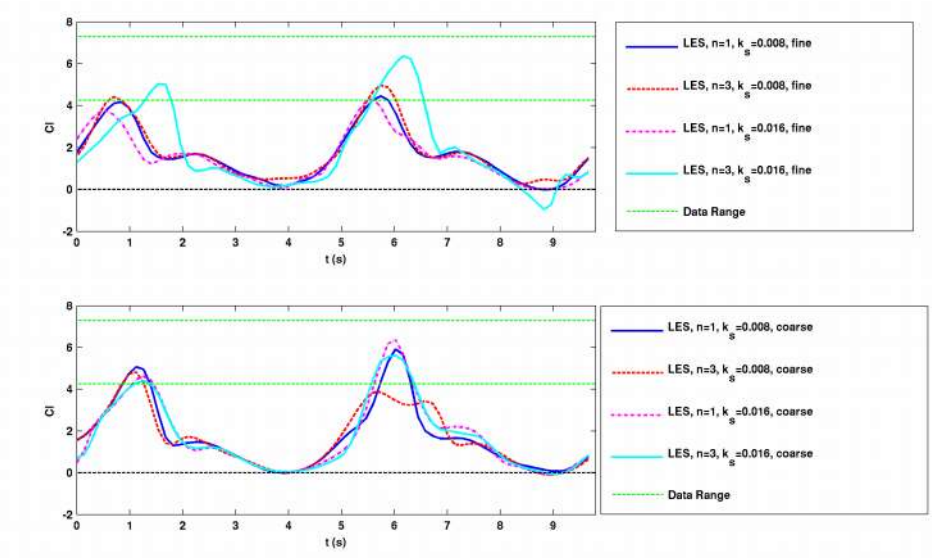

Figure 2: The modeled lift coefficient for the LES models with the fine grid (top panel) and the coarse grid (bottom panel). The legend for each panel is shown on the right of each panel. The range of available laboratory data contained within the two green lines.

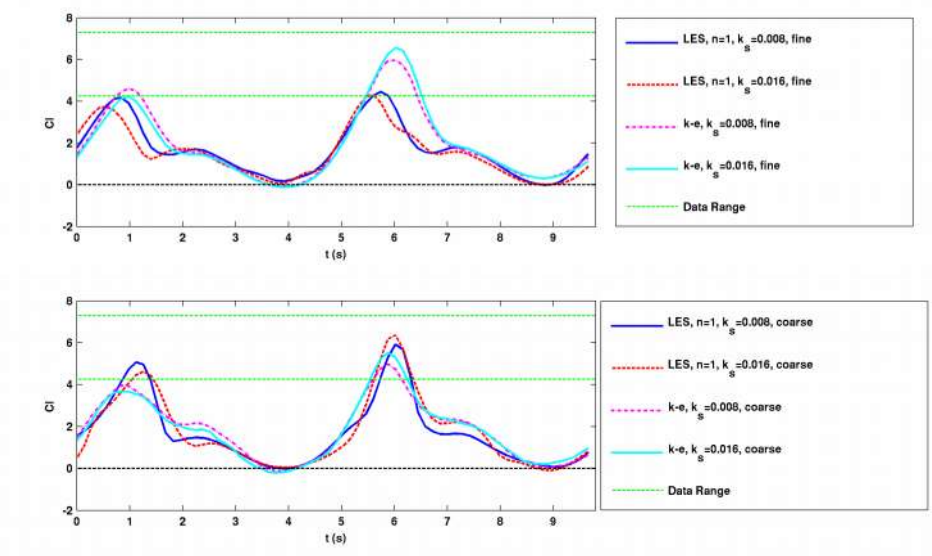

Figure 3: The modeled lift coefficient for the LES $n = 1$ and k-ϵ models with the fine grid (top panel) and the coarse grid (bottom panel). The legend for each panel is shown on the right of each panel. The range of available laboratory data contained within the two green lines.

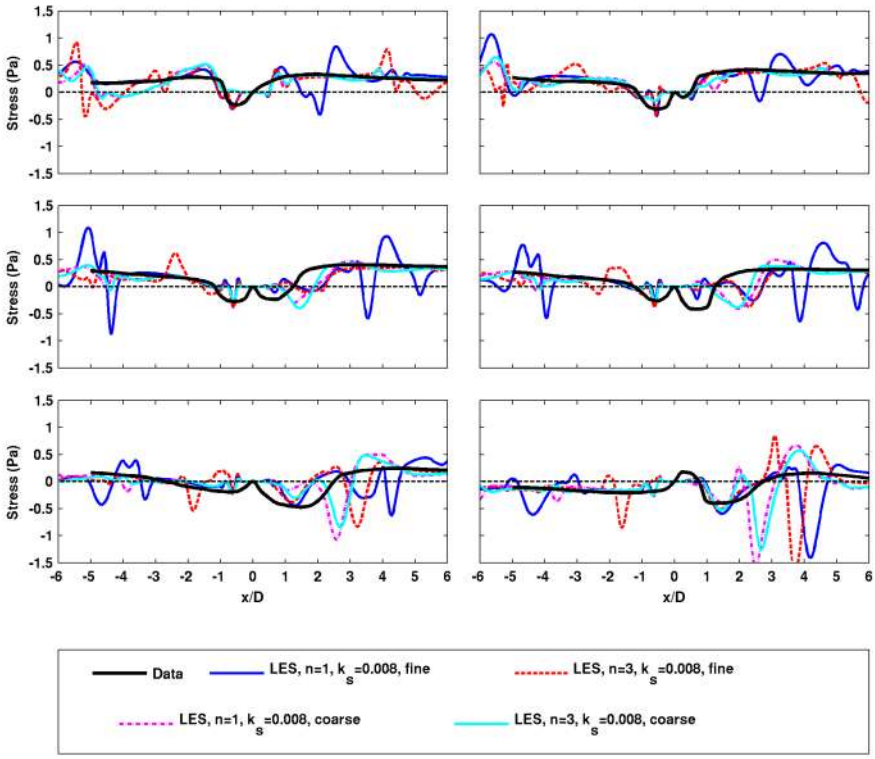

Figure 4: Comparisons of the predicted bed shear stress with the data of Sumer and Fredsøe (1991) (black line). The different LES ($n = 1$, $n = 3$) models and the grid sizes are presented at a roughness of 0.008 cm. The temporal location is given on the bottom right of each panel and matches the time series in Figure 1.

Conclusions

Simulations of the turbulent flow field around a two-dimensional, bottom-seated cylinder were performed under wave forcing conditions. While the model simulations show qualitative agreement with the observations, the quantitative prediction of the vortex characteristics showed variability between closure schemes, obstacle roughness, and grid sizes. The bed stress as a function of wave phase was also examined. The predictions with the LES model were significantly improved over those predicted with the k-ϵ model. Two different near wall van Driest type damping functions were used in the LES model. The $n = 3$, $m = 0.5$ model bed increased the accuracy of the bed stress as compared to the $n = 1$, $m = 1$ damping model.

This work was presented at the 2010 State of the Coast Conference in Baton Rouge, LA.

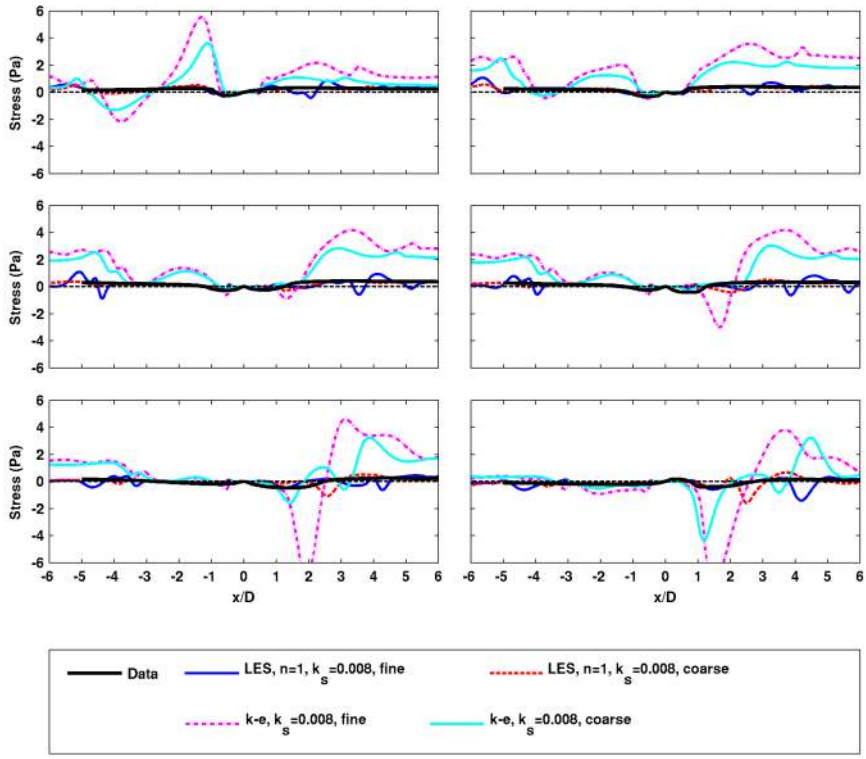

Figure 5: Comparisons of the predicted bed shear stress with the data of Sumer and Fredsøe (1991) (black line). The LES $n = 1$ and k-ϵ models are presented for the two grid sizes for a roughness of 0.008 cm. The temporal location is given on the bottom right of each panel and matches the time series in Figure 1.

References

Bryndum, M. B., Jacobsen, V., and Tsahalis, D. T. (1992). Hydrodynamic forces on pipelines: Model tests. *J. Offshore Mech. Arct.*, 114(4):231–241.

Giri, S. and Shimizu, Y. (2006). Numerical compuation of sand dune migration with free surface flow. *Water Resour. Res.*, 42(W10422):1–19.

Guerts, B. J. (2004). *Elements of Direct and Large-Eddy Simulation*. R. T. Edwards, Inc.

Hirt, C. W. (1993). Volume-fraction techniques: powerful tools for wind engineering. *J. Wind Eng. Ind. Aerod.*, 46-47:327–338.

Li, F. and Cheng, L. (2001). Prediction of lee-wake scouring of pipelines in currents. *J. Waterw., Port, Coastal, Ocean Eng., ASCE*, 127(2):106–112.

Nelson, J. M., McLean, S. R., and Wolfe, S. R. (1993). Mean flow and turbulence fields over two-dimensional bedforms. *Water Resour. Res.*, 29(12):3,935–3,953.

Nelson, J. M., Shreve, R. L., McLean, S. R., and Drake, T. G. (1995). Role of near-bed turbulence structure in bed load transport and bed form mechanics. *Water Resour. Res.*, 31(8):2,071–2,086.

Nichols, C. S. and Foster, D. L. (2007). Full-scale observations of wave-induced vortex generation over a rippled bed. *J. Geophys. Res.*, 112(C10015):1–17.

Richardson, J. E. and Panchang, V. G. (1998). Three-dimensional simulation of scour-inducing flow at bridge piers. *J. Hydraul. Eng., ASCE*, 124(5):530–540.

Sumer, B. M., Chua, L. H. C., Cheng, N.-S., and Fredsøe, J. (2003). Influence of turbulence on bed load sediment transport. *J. Hydraul. Eng., ASCE*, 129(8):585–596.

Sumer, B. M. and Fredsøe, J. (1991). Onset of scour below a pipeline exposed to waves. *Int. J. Offshore Polar*, 1(3):189–194.

Sumer, B. M., Jensen, B. L., and Fredsøe, J. (1991). Effect of a plane boundary on oscillatory flow around a circular cylinder. *J. Fluid Mech.*, 225:271–300.

Sumer, B. M., Jensen, H. R., Mao, Y., and Fredsøe, J. (1988). Effect of lee-wake on scour below pipelines in current. *J. Waterw., Port, Coastal, Ocean Eng., ASCE*, 114(5):599–614.

Tjerry, S. and Fredsøe, F. (2005). Calculation of dune morphology. *J. Geophys. Res.*, 110(F04013):1–13.

Wilcox, D. C. (2002). *Turbulence Modeling for CFD*. DCW Industries, second edition.